Introduction to Physics of X-Ray Bursters

Mari von Steinkirch, steinkirch@gmail.com
University of New York at Stony Brook

April 14, 2014

Contents

Abbreviations

This list is ordered alphabetically by abbreviation.

CNO	carbon-nitrogen-oxygen
EoS	equation of state
HSE	hydrostatic equilibrium
LMXB	low mass X-ray binary
MXRB	massive X-ray binary
qLMXB	quiescent low mass X-ray binary
LTE	local thermodynamic equilibrium
pp	proton-proton
TOV	TolmanOppenheimerVolkoff equation
XRB	X-ray burster
PRE	Photospheric Radius Expansion

Symbols

Symbols

ρ	mass density
P	pressure
L	luminosity
F	flux
F_∞	apparent flux at the infinity (for a remote observer)
g	gravitational acceleration
z_g	surface redshift
T	temperature
T_eff	effective temperature (at surface)
T_eff^∞	effective temperature at the infinity (for a remote observer)
M	mass of the neutron star
R	radius of the neutron star
R_∞	apparent radius of a neutron star for a remote observer
R_bb	Blackbody raduys
f_c	color correction factor
$\odot$	refers to the sun; *e.g.,* , $M_\odot$ for one solar mass
κ_e	Thomson scattering opacity

κ_ν	monochromatic, or frequency dependent, opacity

Constants[1]

c	speed of light; $c = 2.99792458 \times 10^{10}$ cm s^{-1}
G	gravitational constant; $G = 6.67259(85) \times 10^{-8}$ cm^3 g^{-1} s^{-2}
h	Planck constant; $h = 6.6260755(40) \times 10^{-27}$ erg s
$\hbar$	Planck constant over 2π; $\hbar = 1.05457266(63) \times 10^{-27}$ erg s
ρ_0	density of a heavy atomic nucleus; $\rho = 2.8 \times 10^{14}$ g cm^{-3}
m_e	mass of electron; $m_\mathrm{e} = 9.1093897(54) \times 10^{-28}$ g
m_p	mass of proton; $m_\mathrm{p} = 1.6726231(10) \times 10^{-24}$ g
m_n	mass of neutron; $m_\mathrm{n} = 1.6749286(10) \times 10^{-24}$ g
m_H	mass of hydrogen; $m_\mathrm{H} = 1.6733 \times 10^{-24}$ g
λ_c	Compton wavelength; $\lambda_c = h/m_\mathrm{e}c = 0.0243$ Å
k_B	Boltzmann constant; $k_\mathrm{B} = 1.380658(12) \times 10^{-16}$ erg K^{-1}
σ_SB	Stefan-Boltzmann constant; $\sigma_\mathrm{SB} = 5.6705(19) \times 10^{-5}$ erg s^{-1} cm^{-2} K^{-4}
R_S	Schwarzschild radius; $R_\mathrm{S} = 2GM/c^2 \sim 2.95 M/M_\odot$ km
a	radiation density constant; $a = 4\sigma_\mathrm{SB}/c = 7.566 \times 10^{-15}$ erg cm^{-3} K^{-4}
$M_\odot$	solar mass; $M_\odot = 1.9891 \times 10^{33}$ g
σ_T	Thompson cross-section; $\sigma_\mathrm{T} = 6.65 \times 10^{-25}$ cm^2

[1]The constant values were obtained from [WIS14].

Part I

Theoretical Review of Neutron Stars and X-Ray Bursters

Chapter 1

A Brief Story of Light

Silence. The Big Bang starts the universe. For almost 400 thousand years the universe was opaque to the light. During these primordial years, most of the photons in the universe were interacting with electrons and protons in a *photon and baryon fluid*. However, when the baryonic matter in the universe gained free electrons during the period of *recombination*, it became neutral, thereby releasing the photons. This produced the oldest light in the universe, the *cosmic microwave background* (CMB), strong evidence of the Big Bang. When the photons were released (or decoupled), the *universe became transparent* [Pad93][Wei93] [Gut97].

Most information about the universe that reaches our detectors arrives as photons. In Astronomy, the total electromagnetic spectrum is used, consisting of all wavelengths, ranging from very short wavelength gamma rays ($\sim$ 1 Å) and X-rays ($0.1 - 100$ Å) to very long wavelength radio waves. Like all waves, electromagnetic waves carry both energy and momentum in the direction of propagation. Moreover, the study of astrophysical objects, such as neutron stars, is possible due the photons that escape from their *photospheres*. For this reason, we start our journey by briefly introducing the Physics of how light transmits information.

1.1 Light as a Wave and a Particle

In the XVII century, Christian Huygens described light as consisting of *waves*, where the distance between two waves crest is the *wavelength*, λ, and the number of waves per second passing through a point in space is the *frequency*, ν of the wave [Huy90]. The speed of the light wave is related as $c = \lambda\nu$. A demonstration of the wave character of light was

possible through the double-slit experiment, in which monochromatic light from a single source passes through two narrow parallel slits. The light falls upon a screen beyond the slit into a series of interference fringes. This demonstrated the *superposition principle* of light. Where two waves meet, they add algebraically, producing *constructive* or *destructive* interference.

In the XIX century, James Clerk Maxwell stated that the wave equation predicted the existence of electromagnetic wave: transverse wave equations for oscillatory electric and magnetic field vectors [Max61]. A few years later, Heinrich Hertz produced radio waves in his laboratory and confirmed their reflection, refraction, and polarization properties [Her88].

In the beginning of the XX century, Max Planck discovered the empirical formula to fit the *blackbody* spectra together with the beginning of the *quantification* of energy [Pla01]. He assumed that a standing electromagnetic wave could not acquire any arbitrary amount of energy, instead, the wave could have only specific allowed energy values that were integral multiples of a minimum wave energy. This is the quantum of energy given by $E = h\nu$ or $E = hc/\lambda$, where $h = 6.626 \times 10^{-27}$ erg s is the *Planck constant*. Moreover, the energy of an electromagnetic wave was given by $E_{\rm n} = nh\nu$ where n is an integer of the *number of quanta of the wave*.

Despite the wave nature of light, the explanation to the continuous spectrum of radiation led to the complementary *particle description of light*. In 1905, Albert Einstein explained the *photoelectric effect*. This effect is demonstrated when light shines on a metal surface, ejecting electrons [Ein05b]. The kinetic energy does not depend on the brightness of the light shining. Moreover, increasing the intensity of monochromatic light source would eject more electrons but would not increase their kinetic energy. To increase the ejection of electrons, one would have to increase the *frequency* of the light. The energy of a single *photon* of frequency ν is related to the Planck's quantum energy $E_\gamma = h\nu$.

The most convincing evidence that light has a particle-like nature was given a few years later by Arthur Holly Compton [Com23]. He measured the change in the wavelength of X-ray photons when scattered by free electrons. Because photons are massless particles that move at speed of light, the momentum of a photon was related to energy as $E_\gamma = p_\gamma c$. When a photon and a free electron collide, the photon is scattered at an angle θ. The photon loses energy to the electron, and its wavelength is increased by

$$\Delta\lambda \equiv \lambda_{\rm final} - \lambda_{\rm initial} = \frac{h}{m_{\rm e}c}\,(1 - \cos\theta),$$

where $m_{\rm e}$ is the mass of the electron, and $\lambda_c = h/m_{\rm e}c = 0.0243$ Å is

the *Compton wavelength*, the characteristic change in the wavelength of the scattered photon.

The final piece for the wave-particle duality was brought by Louis de-Broglie in that same time [deB24]. He stated that the energy and moment of a photon, $E = h\nu$ and $p = h/\lambda$, could be used to define a frequency and wavelength for *all particles*, not only photons but massive electrons, atoms, etc.

1.2 Intensity of Light and Spectra of Hot Objects

Any object in nature with a temperature above absolute zero emits light of all wavelengths with varying degrees of efficiency. A *blackbody* is an *ideal emitter*, isotropically reflecting as much or more energy at every frequency than any other body at the same temperature. It has a characteristic continuous spectrum, with a shape depending on the temperature. The radiation they emit is called *blackbody radiation*. Star and planets are blackbodies at a first approximation. The *blackbody function* for a specific intensity of nonpolarized blackbody radiation can be given in terms of wavelength:

$$B_\lambda(T) \equiv \frac{2hc^2}{\lambda^5} \frac{1}{e^{\frac{hc}{k_\mathrm{B}\,\lambda\,T}} - 1}, \tag{1.1}$$

or in terms of frequency:

$$B_\nu(T) \equiv \frac{2h\,\nu^3}{c^2} \frac{1}{e^{\frac{h\nu}{k_\mathrm{B}\,T}} - 1}, \tag{1.2}$$

or in terms of *angular frequency*:

$$B_\omega(T) \equiv \frac{\hbar\,\omega^3}{4\pi^3\,c^2} \frac{1}{e^{\frac{\hbar\omega}{k_\mathrm{B}}} - 1}, \tag{1.3}$$

where $k_\mathrm{B} = 1.380658(12) \times 10^{-16}$ erg K^{-1} is the *Boltzmann constant*; $h = 6.6260755(40) \times 10^{-27}$ erg s is the Planck constant; $\hbar = 1.05457266(63) \times 10^{-27}$ erg s is the Planck constant over 2π; and T is the temperature in kelvin. The blackbody temperature is also referred as T_bb when the distinction is needed.

1.2.1 Intensity of Radiation

In the vacuum, a light ray does not spread (or diverge) and the intensity is constant. However, in the presence of matter, the specific intensity varies

with direction. For an isotropic radiation field (with the same intensity in all directions), such as the blackbody radiation, we can calculate the *mean intensity of the radiation* by integrating the specific intensity over all directions, and dividing by 4π sr, the solid angle enclosed by a sphere:

$$\langle B_\nu \rangle = \frac{1}{4\pi} \int B_\nu d\Omega = \frac{1}{4\pi} \int_{\phi=0}^{2\pi} \int_{\theta=0}^{\pi} B_\nu \sin\theta d\theta d\phi. \tag{1.4}$$

1.2.2 Wien's Displacement Law

As the temperature of a blackbody increases, it emits more energy per second across all wavelengths. A blackbody spectrum peaks at a *maximum wavelength* related to the object's temperature by the *Wien's displacement law* [Wie98] [NIS14]:

$$\lambda_{\rm max} T \equiv 2.8977721(26) \text{ cm K}. \tag{1.5}$$

1.2.3 Luminosity

In the end of the XIX century, Josef Stefan and Ludwig Boltzmann showed that the *luminosity*, L (energy emitted per second), of a blackbody of area $A = 4\pi R$ [cm] and temperature T [K] is given by:

$$L \equiv 4\pi R \, \sigma_{\rm SB} \, T^4 \ \ [\text{erg s}^{-1}], \tag{1.6}$$

where $\sigma_{\rm SB} = \pi^2 k_{\rm B}^4 / (60 \hbar^3 c^2) \sim 5.670 \times 10^{-5}$ erg s^{-1} cm^{-2} K^{-4}, is the *Stefan-Boltzmann constant* [Ste79] [Bol84].

To prove this, we calculate the *monochromatic luminosity* assuming that each small patch of the object's surface area, dA, emits blackbody radiation isotropically. The emitted energy per second having frequencies between ν and $\nu + d\nu$ can be obtained by integrating the luminosity through the solid angle $d\Omega = \sin\theta d\theta d\phi$ (yielding π) and area (yielding $4\pi R^2$):

$$\begin{aligned} L_\nu \, d\nu &= B_\nu(T) \, d\nu \cdot dA \cos\theta \cdot d\Omega, \\ L &= 4\pi^2 R^2 \int_0^\infty B_\nu(T) \, d\nu, \\ &= 4\pi^2 R^2 \, \frac{\sigma_{\rm SB} T^4}{\pi} \ \ [\text{erg s}^{-1}]. \end{aligned}$$

1.2.4 Flux and Distance of Sources

The measure of a source's *intrinsic brightness* is linked to its distance. The brightness of a star is measured in terms of the received *radiant flux*, F. The radiant flux is the total amount of light energy of all wavelengths that crosses a unit area oriented perpendicular to the direction of the light's travel in unit time, *i.e.,* the number of ergs of starlight energy arriving per second over one square centimeter of a detector aimed to the star:

$$F \equiv \frac{E}{A\,t} \ \ [\mathrm{erg\,cm^{-2}\,s^{-1}}].$$

The radiant flux received from an object also depends on both its intrinsic luminosity, L (defined in the Eq. 1.6), and its distance from the observer, D. This is also know as the *Inverse Square Law* for light:

$$F \equiv \frac{L}{4\pi D^2} \ = \frac{R}{D^2}\,\sigma_{\mathrm{SB}}\,T^4 \ \ [\mathrm{erg\,cm^{-2}\,s^{-1}}]. \tag{1.7}$$

1.3 The Formation of Spectral Lines

The distinctions between the spectra of stars with different temperatures are due to electrons occupying different atomic orbitals in the atmospheres of these stars. The details of spectral line formation result from the fact that electrons can be found in any of the atom's orbitals and atoms can be in any of various stages of ionization. For this reason, we use statistical mechanics to describe the formation of spectral lines in astrophysical objects.

For a gas in thermal equilibrium, the fraction of particles having a given speed is described by the *Maxwell-Boltzmann distribution function* [Max59]. The number of gas particles per unit volume having a speed between v and $v + dv$ is:

$$n_v\,dv = n\left(\frac{m}{2\pi k_{\mathrm{B}}T}\right)^{3/2} e^{-mv^2/2kT}\,4\pi v^2\,dv, \tag{1.8}$$

where n is the *total number density* (number of particles per unit volume) and m is an individual particle's mass. The exponent is the ratio of a gas particles *kinetic energy*, $1/2mv^2$, to the *characteristic thermal energy*, $k_{\mathrm{B}}T$, [Car96].

Most of the particles do not have an energy much greater or much smaller than the thermal energy, such that the distribution peaks when these energies are at the *most probably speed*, $v_{\mathrm{mp}} = \sqrt{2k_{\mathrm{B}}T/m}$. The high-speed exponential tail of the distribution function results in a higher average temperature, increasing the *root-mean-square* speed, $v_{\mathrm{rms}} = \sqrt{3k_{\mathrm{B}}T/m}$. The

atoms of a gas lose or gain energy as they collide and their distribution in the speeds produces a distribution of the electrons among the atomic orbitals. This distribution is governed by a fundamental result of statistical mechanics that states that orbitals of lower energy are more likely to be occupied by electrons.

To understand how these distributions create the spectrum of a given object, let s_1 stand for the set of quantum numbers that identifies a state of energy E_1 for a system of particles, and let s_2 be the set of quantum numbers that identifies a state of energy E_2. The energy levels of the system may be *degenerate*, with more than one quantum state having the same energy (*e.g.,* $E_1 = E_2$), and each of the degenerate states must be counted separately. To account for the number of states that have a given energy, we can define g_1 to be the number of states with energy E_1, and similarly, g_2 for E_2. These are the *statistical weights* of the energy level.

The ratio of the probability that the system is in the state s_2 to the probability that the system is in the state s_1 is given by [Bol72]:

$$\frac{P(E_2)}{P(E_1)} = \frac{g_2 e^{-E_2/k_{\rm B}T}}{g_1 e^{-E_1/k_{\rm B}T}} = \frac{g_2}{g_1} e^{-(E_2-E_1)/k_{\rm B}T}, \tag{1.9}$$

where the term $e^{-E/k_{\rm B}T}$ is called the *Boltzmann factor*, which explain the relative number of atoms in different stages of ionization.

For a gas at high temperatures, the thermal collisions of the atoms ionize some of the atoms. Electrons that are usually bound to the atom are ejected from the atom and they form an electron gas coexisting with the gas of atomic ions and neutral atoms. This state of matter is called a *plasma*. Since stellar atmospheres contain a vast number of atoms, we can write the ratio of probabilities as the ratio of the number of atoms of a given element in a specified state of ionization:

$$\frac{N_2}{N_1} = \frac{g_2 e^{-E_2/k_{\rm B}T}}{g_1 e^{-E_1/k_{\rm B}T}} = \frac{g_2}{g_1} e^{-(E_2-E_1)/k_{\rm B}T}.$$

Now, let ϵ_i be the ionization energy necessary to remove an electron from an atom in the ground state, from ionization state i to state $i+1$ (*e.g.,* , for hydrogen, the energy needed to convert H_I to H_{II}). An average of all the possible partitioning of orbital energy has to be calculated. This procedure involves finding the *partition functions*, $\mathcal{Z}$, for the initial and final atoms. The partition function is the weighted sum of the number of ways the atom can arrange its electrons. For example, more energetic configurations should receive less weight from the Boltzmann factor when taking the sum. Writing

E_i as the energy of the ith energy level, and g_i as the degeneracy of that level, the partition function is:

$$\mathcal{Z} \equiv g_1 + \sum_{i=2}^{\infty} g_i e^{-(E_i - E_1)/k_{\rm B}T}.$$

The expression that relates the ionization state of an element to the temperature and pressure is given by the *Saha equation* [Sah21]. It describes the degree of ionization of the plasma as a function of the temperature, density, and ionization energies of the atoms. We obtain the Saha equation by using the partition functions $\mathcal{Z}_i$ and $\mathcal{Z}_{i+1}$ for the atom in its initial and final states of ionization (*i.e.,* the ratio of the number of atoms in stage $i+1$ to the number of atoms in stage i):

$$\frac{N_{i+1}}{N_i} = \frac{2\mathcal{Z}_{i+1}}{n_e \mathcal{Z}_i} \left(\frac{2\pi\, m_e\, k_{\rm B} T}{h^2} \right)^{3/2} e^{-\epsilon_i / k_{\rm B} T}, \tag{1.10}$$

where n_e is the number of free electrons, and m_e is the electron mass. The factor 2 is due to the two possible electron spins. A simple observation for this equation is that as the number density of free electron increases, the number of atoms in the higher stage of ionization decreases (since there are more electrons to recombine).

Optionally, we can also express the *pressure* of the free electrons, P_e, using the ideal gas law $P_e = n_e k_{\rm B} T$:

$$\frac{N_{i+1}}{N_i} = \frac{2 k_{\rm B} T \mathcal{Z}_{i+1}}{P_e \mathcal{Z}_i} \left(\frac{2\pi m_e k_{\rm B} T}{h^2} \right)^{3/2} e^{-\epsilon_i / k_{\rm B} T}.$$

1.4 Redshift and Gravitational Redshift

A wave is a disturbance that travels through a medium. In the case of electromagnetic waves, the wave always travel at the same speed in similar medium, *i.e.,* its is independent of the motion of the light source [Ein05a]. Since $c = \lambda\nu$, the effects of motion between two referential should be observed on λ or ν. If an object is moving relative to an observer, the light it emits can be modified by this motion. If the light is moving away, this shift to a longer wavelength, called *redshift*. If the source is moving toward, the shift is for a shorter wavelength, called *blueshift*. A redshift parameter z is used to describe this change:

$$z \equiv \frac{\lambda_{\rm obs} - \lambda_{\rm rest}}{\lambda_{\rm rest}} = \frac{\Delta t_{\rm obs}}{\Delta t_{\rm rest}} - 1. \tag{1.11}$$

where Δt is the time observed between two light wave crest.

The *gravitational redshift* decreases the frequency of the light as it travels upward a distance h:

$$\frac{\Delta\nu}{\nu_0} = -\frac{v}{c} = -\frac{gh}{c^2}.$$

Let us first see the results under weak gravity to show the first-order correction to the frequency of the photon. We can obtain an approximate expression for the *total gravitational redshift* of a beam of light that escapes out to infinity by integrating the above expression from the initial position r_0 to infinity. We use the Newtonian gravity, $g = GM/r^2$, and $h = dr$, for a spherical mass, M, located at the origin, for some local inertial reference frame. By integrating, we add the redshifts obtained for several of different frames. The radial coordinate r can be used to measure distances for these frames if spacetime is nearly flat (*e.g.,* if the radius of curvature is very large compared to r_0). Let ν_0 and ν_∞ be the frequencies at r_0 and infinity, respectively:

$$\int_{\nu_0}^{\nu_\infty} \frac{d\nu}{\nu} \;\sim\; -\int_{r_0}^{\infty} \frac{GM}{r^2c^2}\, dr \longleftrightarrow \ln\Big(\frac{\nu_\infty}{\nu_0}\Big) \;\sim\; -\frac{GM}{r_0c^2},$$

which is valid when gravity is weak ($r_0/r = GM/r_0c^2 \ll 1$). This can be rewritten as :

$$\frac{\nu_\infty}{\nu_0} \;\sim\; e^{-GM/r_0c^2} \;\sim\; -\frac{GM}{r_0c^2}.$$

Nevertheless, for astrophysical objects such as neutron stars, we are interested in the exact result for the gravitational redshift, valid for a strong gravitational field. In this case, we have:

$$\frac{\nu_\infty}{\nu_0} = \Big(1 - \frac{2GM}{r_0c^2}\Big)^{1/2}.$$

The gravitational redshift can be incorporated into the redshift parameter in Eq. 1.11, giving:

$$z_{\rm g} = \frac{\lambda_\infty - \lambda_0}{\lambda_0} = \frac{\nu_0}{\nu_\infty} - 1 = \frac{\omega_0}{\omega_\infty} - 1 = \Big(1 - \frac{2GM}{r_0c^2}\Big)^{-1/2} - 1. \qquad (1.12)$$

This shows the results of the *gravitational time dilation*, *i.e.,* time pass slowly as the surrounding spacetime becomes curved.

To understand the above results, we need to take the curvature of the space into the account. Space will not be flat in the vicinity of a massive

object, requiring a description of the metric of the curved spacetime that will replace the one for a flat spacetime. Albert Einstein realized that the paths followed by freely falling objects through spacetime are geodesics, where mass tells how the spacetime is curved and how spacetime acts on mass, telling it how to move. Any freely falling particle follows the straightest possible worldline, a *geodesic*, through spacetime. For a massive particle, the geodesic has a maximum or a minimum interval, while for light, the geodesic has a null interval. In other words, in a curved spacetime, the *spacetime interval* between two points, $s^2 = \Delta r^2 - c^2\Delta t^2$, along a *timelike geodesic* (*i.e.,* $c^2\Delta t^2 > \Delta r^2$) is an extreme, either a maximum or a minimum, when compared with the intervals of nearby worldliness between the same two events. A massless particle such as photon flows a *null geodesic* (lightlike interval) with:

$$\int \sqrt{(ds)^2} = 0.$$

In spherical coordinates, the metric between two nearby points in flat space is $(dl)^2 = (dr)^2 + (rd\theta)^2 + (r\sin\theta d\phi)^2$, thus the corresponding expression for the flat spacetime metric is:

$$(ds)^2 = (cdt)^2 - (dr)^2 - (rd\theta)^2 - (r\sin\theta d\phi)^2.$$

The metric that describes the curved spacetime surrounding a spherical mass, M is giving by the solutions of the *Einstein field equation*. For instance, the *Schwarzschild metric* is a vacuum solution (the only spherically symmetric vacuum solution), and it is valid only in the empty space, outside the object:

$$(ds)^2 = \left(c\,dt\sqrt{1-\frac{2GM}{rc^2}}\right)^2 - \left(\frac{dr}{\sqrt{1-2GM/rc^2}}\right)^2 - (rd\theta)^2 - (r\sin\theta d\phi)^2. \tag{1.13}$$

We see that for a curved space, the factor $\sqrt{1-2GM/rc^2}$ plays a role in the metric: the curvature of space resides in the radial term. The angular terms are the same as those for flat spacetime. Therefore, the radial distance measured simultaneously ($dt = 0$) between two nearby points on the same radial line ($d\theta = d\phi = 0$) is just the proper distance:

$$d\mathcal{L} = \sqrt{-(ds)^2} = \frac{dr}{\sqrt{1-2GM/rc^2}},$$

and the spatial distance $d\mathcal{L}$ between two points on the same radial line is greater than the coordinate difference dr.

Finally, the Schwarzschild metric also incorporates time dilation and the gravitational redshift (two aspects of the same effect):

$$d\tau = \frac{ds}{c} = d\tau\sqrt{1 - \frac{2GM}{rc^2}},$$

since $d\tau < dt$, this shows that times passes more slowly when closer to the mass M [Mis73].

Chapter 2

Formation and Basic Properties of Neutron Stars

The final stages of stellar evolution result in the production of a *white dwarf*, or a *neutron star*, or a *black hole*. These compact objects are formed when nuclear fusion in the stellar core fails to produce sufficient radiation pressure to support the star, resulting on the core collapsing under its own gravity. Low mass stars end their evolution as a white dwarf, while more massive stars become supernovae and leave behind a neutron star or a black hole.

The main objective of this thesis is to be able to understand some properties and underlying principles of neutron stars' atmospheres. Neutron stars are the most compact (densest) *stellar remnant* that have a boundary (*i.e.,* that can be observed). They have a typical mass of $M \sim 1 - 2M_{\odot}$, where $M_{\odot} = 1.9891 \times 10^{33}$ g (solar mass). Their radii are extremely small, ranging $R \sim 10 - 13$ km [Pot14]. The density of neutron stars is in average $\bar{\rho} \sim 10^{15}$ g cm^{-3}, which is a few times larger than the typical densities of heavy atomic nucleus, $\rho_0 = 2.8 \times 10^{14}$ g cm^{-3}. The extreme physical conditions of the matter encountered inside neutron stars cannot be reproduced in any terrestrial laboratory, which makes the study of these objects extremely important to reveal the underlying Physical laws and to test the general theory of relativity. There are several theoretical models possible to describe the equations that govern the interior of neutron stars, and a definitive solution is still not available [LP01].

2.1 Birth and Life of Neutron Stars

To maintain its luminosity, a star must have sources of energy contained within, either nuclear or gravitational. With the depletion of hydrogen in the core, the generation of energy via the *pp*-chain must stop. However, the core temperature has increased to the point that the nuclear fusion continues to generate energy in many different compositions shells. For an *isothermal* core to support the material above it in *hydrostatic equilibrium*, the required gradient must be the result of a continuous increase in density in the center of the star. The mass of an isothermal core can be increased if an additional source of pressure can be found to supplement the ideal gas pressure. This occurs if the electrons in the gas becomes degenerate. When the density of a gas becomes sufficiently high, the electrons in the gas must occupy the the lowest available energy levels. Since electrons are fermions, they start occupy progressively higher energy states. In the case of complete degeneracy, the pressure of the gas is due to the nonthermal motions of the electrons, and it becomes independent of the temperature of gas. If the electrons are nonrelativistic, the pressure of a complete degenerate electron gas is given by $P_e \propto \rho^{5/3}$.

Completing the main-sequence phase of stellar evolution, a sequence of evolutionary stages which involve nuclear burning happens in the cores of stars, together with nuclear burning in concentric mass shells. At various times, core burning in a mass shell may cease, accompanied by a readjustment of the structure of the star. This readjustment may involve expansion or contraction of the envelopes and the development of convection zones, until the core begins to collapse. The destiny of the star now is defined by its mass.

2.1.1 The Chandrasekhar Limit

The *Chandrasekhar limit* is the maximum mass of a stable white dwarf star. First, a relation between the radius and mass of these objects can be found using an estimate of the central pressure to the electron degeneracy pressure [Car96]:

$$\frac{2}{3}\pi\, G\, \rho^2\, R^2 \;=\; \frac{(3\pi^2)^{2/3}}{5}\,\frac{\hbar^2}{m_e}\left[\frac{Z}{A}\frac{\rho}{m_H}\right]^{5/3},$$

where $m_{\rm H}$ is the hydrogen mass. Assuming constant density, $\rho = M/(4/3\pi R^3)$, leads to an estimate of the radius:

$$R_{\rm Chandra} \sim \frac{(18\pi)^{2/3}}{10} \frac{\hbar^2}{G\, m_e\, M_{\rm Chandra}^{1/3}} \left[\frac{Z}{A}\frac{1}{m_H}\right]^{5/3}.$$

The volume of the object is inversely proportional to its mass, so more massive objects are actually smaller. The electrons must be closely confined to generate the larger degeneracy pressure required to support a more massive star. The limit to the amount of matter that can be supported by electron degeneracy pressure is then (the electron speed is changed to $v = c$):

$$P = \frac{(3\pi^2)^{1/3}}{4}\hbar c \left[Z/A\frac{\rho.}{m_H}\right]^{4/3},$$

Approaching the Chandrasekhar limit leads to the collapse of the degenerate core, resulting in a *Type II supernova*. This limit can give the maximum mass by equating this equation to the estimate of central pressure.

2.1.2 Neutronization

If the initial mass of the star on the main sequence was not too large ($M < 35M_\odot$) the remnant in the inner core will stabilize and become a neutron star, supported by degenerate *neutron pressure*. If the initial stellar mass is much larger, even the pressure of neutron degeneracy cannot support the remnant against the pull of gravity, and the final collapse can produce a black hole [Hea80].

Because neutron stars are formed when the degenerate core of an aging supergiant star nears the Chandrasekhar limit and collapses, a typical neutron star mass contains $M \sim 1.4M_\odot/m_n \sim 10^{57}$ neutrons. Its nucleus has a mass number of A $\sim 10^{57}$, that is held together by gravity and supported by neutron degeneracy pressure:

$$R_{\rm NS} \sim \frac{(18\pi)^{2/3}}{10} \frac{\hbar^2}{G M_{\rm NS}^{1/3}} \frac{1}{m_{\rm H}^{8/3}}.$$

At $\rho \sim 10^6$ g cm^{-3}, the electrons become relativistic. The minimum energy arrangement of protons and neutrons changes since the energetic

electrons can convert protons in the iron nuclei into neutrons by the process of electron capture:

$$p^+ + e^- \rightarrow n + \nu_e.$$

Because the neutron mass is slightly greater than the sum of the proton and the electron masses ($m_{\rm n}c^2 - m_{\rm p}c^2 - m_{\rm e}c^2 = 0.78$ MeV), the electron must supply the kinetic energy for the difference.

The density must be larger than $\rho = 10^9$ g cm^{-3} for the protons in iron nuclei to capture electrons. The most stable arrangement of nucleus is with neutrons and protons in a lattice of neutron-rich nuclei, *i.e., neutronization*. In general, these neutrons would revert to protons via *β-decay*, however since the electrons are completely degenerate, there are no vacant states for emitted electrons, thus the neutrons cannot decay back into protons.

When the density reaches $\rho \sim 4 \times 10^{11}$ g cm^{-3}, the minimum-energy arrangement is one where some of the neutrons are free, outside the nuclei. The result of two fermions coming together is a boson, and so is not subject to the *Pauli exclusion principle*. Degenerate bosons can all be in the lowest energy state, and the fluid of paired neutrons cannot lose any energy. It is a *superfluid* that flows without resistance (no viscosity).

As the density increases further, the number of free neutrons increases as the number of electrons declines. The neutron degeneracy pressures exceeds the electron degeneracy pressure when the density reaches $\rho \sim 4 \times 10^{12}$ g cm^{-3}. As the density approaches the density of the nuclei, they dissolve and there is no distinction between neutrons inside or outside of nuclei. This fluid is a mixture of free neutrons, protons, and electrons, all dominated by neutron degeneracy pressure (the ratio $n : p : e$ is about $8 : 1 : 1$).

During the first day, the neutron stars cool by emitting neutrinos by *Urca process*:

$$n \rightarrow p^+ + e^- + \bar{\nu}_e$$

$$p^+ + \bar{e} \rightarrow n + \nu_e$$

This process can continue as long as the nucleons are not degenerate, and it is suppressed after the protons and neutrinos settle into the lowest unoccupied energy states. The degeneracy occurs about one day after the formation of the neutron star, when the temperature dropped to $T \sim 10^9$ K. The neutron star is a few hundred years old when its internal temperature declined to $T \sim 10^8$ K, with a surface temperature of several million kelvins. The surface temperature will be around $T_{\rm eff} \sim 10^6$ K for a few thousand years. The blackbody luminosity of an $1.4 M_\odot$ neutron star with this surface temperature shows that the primary radiation is in the form of *X-rays*.

2.1.3 Anatomy of a Neutron Star

With exception of the detection of neutrinos, there is no direct way to observe the central regions of neutron stars. Nevertheless, as we have seen above, stellar evolution is the result of a constant fight against the inward pull of gravity by the outward force of radiation pressure. Using physical principles, we can generalize the anatomy of a neutron star into five parts [Sea83] [Pot14]:

Core: Density of $\rho \sim \rho_0 \sim 10^{15}$ g/cm^3. The composition of the superdense matter in the core remains uncertain. It may contain quark gluon plasma or more exotic forms of matter. The composition of the star's deep interior varies according to the physics of the equation of state assumed.

Neutron Fluid: Density of 10^{14} g/cm^3 $< \rho \leq \rho_0$. Thickness is on the order of 10 kilometers. Composed of a neutron superfluid in equilibrium to a small superfluid of protons and electrons.

Inner Crust: Density of 4.3×10^{11} g/cm^3 $< \rho \leq 10^{14}$ g/cm^3. Thickness is on the order of one kilometer. Composed of a lattice of neutron rich nuclei coexisting with a superfluid of neutron gas and electron gas.

Outer Crust: Density of 10^6 g/cm^3 $< \rho \leq 4.3 \times 10^{11}$ g/cm^3 (the boundary lies at the critical *neutron-dip density* [PGC11]). Thickness is on the order of one kilometer and it is composed of a solid Coulomb lattice of heavy nuclei (*e.g.,* iron), and degenerate gas. Absence of free neutrons.

Photosphere: Density of $\rho \leq 10^6$ g/cm^3. Thickness is on the order of centimeters. The source of the observed thermal radiation, which is dependent on the temperature, surface gravity, and magnetic field.

The composition of neutron star surfaces is unknown, and neutron stars in different environments could have different atmospheric conditions. Spectra generated by atmospheres of many different compositions will be different from blackbody or *grey-body emission*, and this is one of the objects of study in this work.

2.2 Properties of Neutron Stars

2.2.1 Mass and Radius

The masses of neutron stars are of theoretical interests for two main reason. First, they place constraints on nuclear physics (determining the equation of state of matter at extremely high temperatures) and the general relativity theory (the equation of state governs the limiting mass of a stable neutron star). Second, as we have seen above, when it comes to the study of stellar evolution, highly massive stars develop a degenerate core that grows by accretion of mass from the surrounding stellar envelope. As the mass of this core approaches the Chandrasekhar limiting mass, $M_{\rm Chan} \sim 1.4 M_{\odot}$, a thermonuclear runaway and collapses can lead to a supernova and in some cases to the production of a neutron star. The mass of this newborn neutron star is comparable to that of its progenitor. If a large fraction of observed neutrons stars are found near to $M_{\rm Chan}$, the stellar evolution theory is supported [Jos76].

The radius of a neutron star, R, is determined by the equatorial length $2\pi R$. This is related to the mass, M, and they can be obtained by a solution of the *hydrostatic equilibrium equation* for a given *equation of state* (EoS). The EoS defines the relation of dependence between pressure, P; density, ρ; and temperature, T. A condition of hydrostatic stability is that the density at the stellar center has to increase with mass. Since the pressure in the interior of neutron stars is mainly due by highly degenerate *fermions*, with *Fermi energies* $\epsilon_{\rm F} \gg k_{\rm B}T$, the calculations of R and M are independent of the temperature in the core.

2.2.2 Magnetic Fields and Photospheric Opacities

Magnetic field environments of neutron star atmospheres can be many orders of magnitude large than any value we are able to produce in terrestrial scales. The order of magnitude estimate is about $B \sim 1-4\times10^{12}$ G [Pot14]. These values are still below theoretical limits, of the order of $B_{\rm max} \sim 10^{18-19}$ G, which are obtained by equating the gravitational energy of the star to its electromagnetic energy [CF53].

In stellar atmospheres, radiation interaction with matter is described in terms of *opacities*. These opacities take into account the absorption and scattering cross sections per unit of mass in the system, as we will describe in future chapters.

In *partially ionized photospheres*, the magnetic field can have a strong

effect on opacity. Because of the high density of neutron star photospheres, highly excited states do not survive because of their low binding energies (*pressure ionization* is the process that make bound states vanish with the increase of density).

In this thesis we show many results of neutron stars atmosphere modeling, *i.e.,* their radiation spectra. Zavlin et al. [Zea96] showed the conditions that make it possible to calculate the neutron star spectrum without accounting with the magnetic field. Opacities of *fully ionized atmospheres* do not depend on magnetic field at the frequencies ω that are much larger than the *electron cyclotron frequency*, $\omega_{\rm c}$. This correspond to the energies $E_{\rm c} \equiv \hbar\omega_{\rm c} \sim 11.6 \times 10^{12}$ keV. Thus, for energies that correspond to the maximum of a thermal spectrum,

$$E_{\rm thermal} \;=\; \hbar\omega \;\sim\; (1-10)\, k_{\rm B}T,$$

we are able to neglect the magnetic field effects on opacities if:

$$B \;\ll\; \frac{m_{\rm e}c}{\hbar e}\, k_{\rm B}T \;\sim\; 10^4\, T \;\; [G].$$

In this thesis we analyze the atmospheric models of *quiescent low-mass X-ray binaries* (*i.e., cooling X-ray bursters*, refer to next section). They are neutron stars that produce X-ray bursts, rather than pulses. This indicate that their magnetic fields are weak or negligible. The observed spectrum of X-ray bursters, with their evolution during the long burst and posterior relaxation, are successfully interpreted with nonmagnetic atmosphere models [Pot14] [Sul10].

2.2.3 Effective Temperature and Blackbody Radius

The blackbody function can be used to make connection between the observed properties of a star (*e.g.,* the intensity of photons we see, *i.e.,* the *radiant flux*) and its intrinsic properties (*e.g.,* radius or temperature).

A typical spectral analysis of a stellar object is made by calculating the temporal variation of the blackbody temperature, $T_{\rm bb}$, the (bolometric) flux, F, and the blackbody radius, $R_{\rm bb}$. From Eq. 1.7, the radius of such a blackbody emitting a flux at a distance D, is:

$$R_{\rm bb} = D\left[\frac{F}{\sigma_{\rm SB}T_{\rm bb}^4}\right]^{1/2}. \tag{2.1}$$

This quantity can be calculated if the distance is known, and with measurements of the bolometric fluxes and the blackbody temperatures.

Neutron stars have spectra that are observationally shaped by a blackbody function, but they look *harder* than a blackbody at the *effective temperature* of the atmosphere. The effective temperature of an object, $T_{\rm eff}$, is defined as the total radiative flux, F, going through 1 cm^2 at the surface of this object [BV81].

In the case of spherical neutron stars, R can be taken as their radii. Thus, the temperature at their surfaces, $T = T_{\rm eff}$, is calculated from Eq. 1.6:

$$T_{\rm eff} = \left[\frac{L}{4\pi R^2 \sigma_{\rm SB}}\right]^{1/4}. \tag{2.2}$$

In the following chapters, when we learn about *X-ray bursters' decays*, we will see that we can compose a diagram of $\log F$ versus $\log k_{\rm B} T_{\rm bb}$. In this case, as a result, the value of $R_{\rm bb}$ is approximately constant (*i.e.,* the cooling track is a straight line), proportional to the (*color*) corrections for the effective temperatures and the redshift for the *surface gravity* (defined below).

2.2.4 Compactness and Surface Gravity

The *compactness* parameter of an astrophysical object is given by:

$$c_{\rm g} = \frac{R_{\rm S}}{R}, \tag{2.3}$$

where $R_{\rm S} = 2GM/c^2 \sim 2.95 M/M_\odot$ km is the *Schwarzschild radius* (Eq. 1.13).

While the compactness parameter of a star such as the Sun is $c_{\rm g,\,\odot} \sim 10^{-5}$, the compactness parameter of a typical neutron star is $c_{\rm g,\,NS} \sim 0.2 - 0.5$. When an object has a large compactness parameter, the general relativistic effects become non-negligible.

Nevertheless, as long as the neutron star atmosphere is *geometrically thin*, the only gravitational effect that is relevant for their study is the *surface gravity*. We can write the gravity at the neutron star surface as:

$$g = \frac{GM}{R^2\sqrt{1-c_{\rm g}}} = \frac{GM}{R^2}(1+z_{\rm g})\ [{\rm cm\ s^{-2}}], \tag{2.4}$$

with the redshift parameter, $z_{\rm g}$, given by Eq. 1.12, or by:

$$z_{\rm g} = (1-c_{\rm g})^{-1/2} - 1. \tag{2.5}$$

As a consequence of the surface gravity, the proprieties of the emitted radiation as seen by an observer on the neutron star surface, including luminosity and the effective temperatures, will be different from those measured by an observer far from the surface. The thermal spectrum for a temperature $T_{\rm eff}$ at the surface (Eq. 2.2), is seen by a remote observer as a lower temperature:

$$T_{\rm eff,\infty} = \frac{T_{\rm eff}}{(1+z_{\rm g})}. \tag{2.6}$$

The *apparent radius* of a neutron star for a remote observer is given by:

$$R_\infty = R(1+z_{\rm g}). \tag{2.7}$$

The *apparent photon luminosity* for the effective temperature at the surface (Eq. 1.6) is:

$$L_\infty = \frac{L}{(1+z_{\rm g})^2} = 4\pi\,\sigma_{\rm SB} R_\infty^2\, T_{\infty,\rm eff}^4. \tag{2.8}$$

Assuming that the emission is isotropic (which may not be the case), we can convert flux directly from luminosity (Eq. 1.7):

$$F_\infty = \Big(\frac{R_\infty}{D}\Big)^2 \sigma_{\rm SB}\, T_{\infty,\rm eff}^4. \tag{2.9}$$

2.2.5 Simultaneous Measurements of the Mass and the Radius

Using Discrete Features in the Spectra

If a *discrete feature* (a spectral line) were present and identified in a spectrum, one would have a direct measurement of the gravitational redshift of the neutron surface and thus the ratio M/R. First, by relating the Eqs. 2.4 and 1.12, we have:

$$M = \frac{g^2R^3}{c^2G}\left[\Big(1+\frac{c^4}{g^2R^2}\Big)^{1/2} - 1\right]. \tag{2.10}$$

Proof. Solving for the two equations, gives a quadratic equation for M:

$$\begin{aligned} g &= \frac{GM}{R^2}\Big(1-\frac{2GM}{Rc^2}\Big)^{-1/2}, \\ g^2\Big(1-\frac{2GM}{Rc^2}\Big) &= \frac{GM^2}{R^4} \\ M^2 &= \frac{2g^2R^3}{Gc^2}M - \frac{g^2R^4}{G^2} = 0, \end{aligned}$$

which solution gives the desired result. □

A simultaneously measurement of $z_{\rm g}$ and $R = R_\infty(1+z_{\rm g})^{-1}$ would completely solve Eq. 2.10[1]:

$$M = \frac{c^2}{2G} R_\infty (1+z_{\rm g})^{-1}\Big[1-(1+z_{\rm g})^{-2}\Big]. \tag{2.11}$$

Using the Effective Temperature at Surface

In the next section we will learn about neutron stars with thermal spectra. We can approximate neutron stars to blackbodies[2], described by the Eq. 1.3, to find an approximate relationship between M and R. In this case, using the Wien's displacement law from Eq. 1.5, the position of the spectral maximum is defined as $T_{\rm eff,\infty}$, the effective temperature at the surface of the neutron star. A second measurement is given by the total bolometric flux of the neutron star. These two quantities can be plugged into with Eq. 2.9, if the star is located at a known distance D, to find R_∞.

Spectral modeling of neutron stars is the main study performed in this thesis. It includes solving the equations of hydrostatic equilibrium, energy balance, and radiative transfer. Coefficients of these equations depend on the chemical composition of the atmosphere, effective temperature at the surface, surface gravity, and magnetic field. With the known shape of the neutron star spectrum, we can calculate F and evaluate R_∞. A simultaneous evaluation of $z_{\rm g}$ (*e.g.,* by identification of spectral features) naturally leads to the calculation of M.

Nevertheless, the neutron star spectra may depend on other parameters. For example, the spectrum should be modified by the absorption of interstellar matter, when the photons are traveling through space. In addition, the temperature distribution is not guaranteed to be uniform over the entire neutron star surface. These corrections are beyond the studies of this thesis.

[1]The quantity observed is R_∞/D, determined from the bolometric flux. However, D is usually uncertain.

[2]The approximation is to a *diluted* blackbody, which will demand the calculation of the *color correction factors*, as we will see in the following chapters.

Chapter 3

Neutron Stars with Thermal Spectra

Neutron stars can be divided into *accreting* objects and *isolated* objects. The former accretes matter from a companion and can have transient active accreting periods alternating with *quiescent* periods (when the accretion stops). The radiation from the accreting neutron stars is due to the matter being accreted, forming a hot boundary layer at the surface. Nevertheless, a great part of the radiation from isolated neutron stars and from the transients in quiescence period originates at the surface or in the atmosphere (the transparent layers of gas overlying the opaque interior). In this chapter we review the classes of neutron stars that can be probed by radiation, or the neutron stars' thermal spectra.

A stellar atmosphere is the plasma layer in where the electromagnetic spectra forms, and from where the radiation escapes into space. Photons come from these layers, releasing the energy produced by the thermonuclear reactions in the source's center. Stellar atmospheres are divided into a lower part, the *photosphere*, where radiative transfer dominates, and the upper part, where the temperature is determined by processes other than radiation transfer. This last is not found in neutrons stars, thus we do not discriminate between atmosphere and photosphere in these objects [Pot14].

The thermal spectra of neutron stars contain information about the chemical composition, the temperature at the surface ($T_{\rm eff}$), the magnetic field, the mass, and the radius[1]. To interpret this spectrum we must under-

[1]The spectrum of a neutron star in general include contributions caused by different processes than the thermal emission: processes in pulsar magnetospheres, pulsar nebulae, etc., which are beyond the scope of this work.

stand how light travels trough these layers of gas, and this will be the focus of the next chapter.

3.1 X-ray Bursters

In the 1970's, with the launch of the *Uhuru* satellite, astronomers noted that short bursts of X-ray were being emitted by sources near to center of our galaxies or in *globular clusters* [Lew81]. The *Uhuru Catalog*, issued in four versions with the last being the 4U, was the first comprehensive X-ray catalog. It contained 339 X-ray sources and covered the whole sky in the 2-20 keV energy band [Fea78].

The X-ray bursts were first observed to be neither isolated or nor of any fixed schedule. They rather appeared on irregular intervals from several hours to days. They released great amounts of X-rays, reaching their maximum intensities ($E_{\text{released}} \sim 10^{39}$ ergs), with the surface reaching a temperature of $T_{\text{eff}} \sim 3 \times 10^7$ K (the double of Sun's central temperature), in a few seconds (equal to the energy emitted by the Sun at all wavelengths in two weeks). After this, they would fade to a steady form.

For instance, one of the sources observed at that time by Uhuru, 4U 1820-30 near to the globular cluster NGC 6624, was reported to show two intense X-ray bursters with less than one second of rise times and peak luminosities 20 times larger than the quiescent luminosity. The source also showed an exponential decay of only a few seconds. The cause of these short busters was soon attributed to thermonuclear burning in an accreted material in the surface of a neutron star [WT76] [Hor75] [Cav77]. It was pointed out that the nuclear energy coming outward from the surface layers (due the nuclear burning in the interior layers) would be independent of the source of energy that was being radiated directly from the neutron star's *photosphere* (due the burning of the accreted material and the strong surface gravity on these particles) [Ros73]. In addition, it was shown that the nuclear burning of these accreted particles should be unstable and lead to thermonuclear flashes. This would be caused by unstable burning of a several meters thick layer of accreted hydrogen and helium on the surface of neutron stars from a binary companion. The energy of these flashes could produce variable X-ray emission from the neutron star, but with shorter times than the time scales of the known *X-ray pulsars* at that time [Hor75].

Nowadays we see that X-ray bursters are observed to exhibit a large variety of shapes. They can show spiky peaks, shoulders, and tails, and some show all of these features. Burst from different sources usually look

different, and burst from one source usually seem similar [Bil00] [vdHea04] [Lew77]. In the rest of this chapter we discuss the many classes of X-ray bursters, focusing on the thermonuclear Type I X-ray busters, in general found in *low-mass binary systems*. These objects' atmospheres are the main subject of study in this thesis. For more in depth overviews about X-ray bursters, please see the following review articles: [Lew81] [Lew77] [Jos80] [Lew93] [Bil00] [SB03].

3.1.1 Type I X-ray Bursters

In a *semidetached system* containing a neutron star, hot gas is transferred through the inner *Lagrangian point* from the distended atmosphere of the companion star. Due the energy released when the gas falls down the deep gravitational potential well onto the compact object, many of these systems emits huge quantities of X-rays. The gravitational energy released from matter accreted into a neutron star of mass M and radius R is:

$$E_{\rm grav} \equiv \frac{GMm_{\rm p}}{R} \sim 200{\rm MeV},$$

per nucleon, where $m_{\rm p}$ is the mass of the proton. This is much more than the energy released from thermonuclear fusion,

$$E_{\rm nuc} \sim 5{\rm MeV},$$

per nucleon. Thus, the disparity in efficiency of energy release shows that the neutron star must store power for enough accreted fuel, until the conditions are met to explosively burn. The burning of the accumulated material in the neutron star atmosphere occurs in radially thin shells, and so it is susceptible to *thermal instabilities*. The evidences of this instability was shown with the discovery of *Type I X-ray bursters* with *low-accretion rate* neutron stars [Bil00].

Type I X-ray bursters are accreting neutron stars in **close binary systems**, which produce X-ray bursts with intervals from hours to days (fuel accumulation) followed by a thermonuclear runaway that burns the fuel in 10-100 seconds [Lew77] [Bil00]. After that, they exhibit a *spectral softening* as they decay [vP78].

The burst happens when the accretion column produces a hot spot: the accreted matter is mostly consisting of hydrogen and helium, and piles up on the surface, until reaching the densities and temperatures of a thermonuclear burst (hours to days). When a layer of hydrogen a few meters thick accumulates on the surface, a shell of helium burning ignites below that. This

fusion of helium is explosive and the resulting blackbody spectrum peaks at X-ray wavelengths. Some of the X-rays may be absorbed by the accretion disk and re-emitted as visible light, so an optical flash is sometimes seen a few seconds after the X-ray burst.

As the burst luminosity declines in a matter of seconds, the spectrum matches that of a cooling blackbody with a radius of $R \sim 10$ km, consistent with the presence of a neutron star. During the intervals between bursts, the object's atmosphere does not differ from the atmosphere of a cooling neutron star, where the observed X-ray radiation arises from transformation of gravitational energy of accreting matter into thermal radiation. During this decline, the radiation comes from the heat that was formerly deposited in the crust (during the active period). The *soft X-ray transients* that have recently turned into quiescence can be used to probe the state of the neutron star crust by the decline of $T_{\rm eff}$. After a time that can vary from a few hours to a day or more, another layer of hydrogen accumulates and another X-ray burst is triggered.

3.1.2 Type II (Accretion Instabilities) X-ray Bursters

Type-II X-ray bursters are referred as *rapid bursters* since they recur more frequently than Type I, usually on the time scales of minutes or seconds. Up to a thousand bursts can be seen per day. These bursters are less energetic and they do not show the spectral cooling during the decay, as seen in the Type I. They are caused by gravitational instabilities of the accretion matter, not by thermonuclear reactions, *i.e.,* the burst source is the gravitational potential energy [Wam79] [Pot14]. Type II X-ray bursters will not be of interest in this work.

3.2 Binary X-ray Bursters

As a binary X-ray system reaches the end of its evolution, the secondary star will end up as a white dwarf star, neutron star, or black hole. The effect on the system depends on the mass of the secondary star. Astronomers have identified two classes of binary X-ray systems:

- Systems in which the accretion flow onto a compact object occurs in sporadic bursts with X-ray emission [vP78]. The compact object can be a white dwarf, a neutron star, or a black hole. These systems are usually youthful, being born only a few million years ago in interstellar gas clouds [vdHea04]. As such, these pulsating massive X-ray binaries

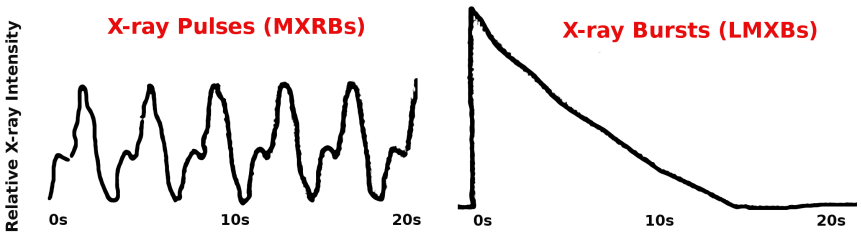

Figure 3.1: This figure shows a pictorial comparison of the profiles of massive X-ray bursters and low-mass X-ray bursters, based on [vdHea04]. A neutron star in a young massive binary system (for example, Centaurus X-3) emits pulses as it rotates (left). A neutron star in low-mass binary systems (for example, 4U 1820-30), have X-ray bursters that occur sporadically, as the accreted material onto the surface goes to thermonuclear detonation (right).

tends to concentrate in the plane of the Milky Way, but not towards the galactic center. Systems with higher-mass secondaries are called *massive X-ray binaries* (MXRBs). In MXRBs, the companion may explode as a supernova [JKR01]. If more than half of the system's mass is retained, a pair of neutron stars will circle each other in orbits that probably have been elongated by the process.

- Systems in which the X-ray burst is caused by thermonuclear flashes in freshly accreted material onto a neutron star surface [vP78]. These systems are usually located in the central bulge of the galaxy and in globular clusters [vdHea04]. These are regions with older stars, around 5-13 billions of years. Since the neutron star accretes matter from a less massive star (*e.g.,* a main sequence star or a white dwarf) in these systems, they are called *low-mass X-ray binaries* (LMXBs). In LMXBs, the companion star will become a white dwarf without disturbing the circular orbit of the system. These systems do not exhibit pulsations.

3.2.1 LMXBs and qLMXBs

About a quarter of LMXBs are found within globular clusters, where there is a high number of stars, making the gravitational capture of a neutron star more likely. The neutron stars in LMXBs may also have been formed by the *accretion-induced collapse* of a white dwarf. In some of LMXBs, periods of large accretion alternate with longer (months to years) periods of

quiescence (when accretion stops). In these quiescent periods, these objects are named quiescent-LMXBs (qLMXBs), and the X-ray radiation comes from the heated surface of the neutron star [Pot14]. Because low-mass stars are small, the two stars must orbit more closely if mass is to be transferred from one star to other. For this reason, the LMXBs have short orbital periods, from days to minutes[2].

The visible-light spectra of the aged X-ray binaries is not similar to those of normal stars. They grow brighter toward the blue end of the spectrum and some of their radiation emerges at distinct wavelengths. Such a spectrum would be produced by an in-flowing disk of gas heated by intense X-ray streaming from inner parts of the disk, right above the neutron star surface. Emission from the disk almost completely washes out the light from the companion star. That disparity implies that the companion must be faint, with mass no great than the Sun.

The LMXBs' occasional bursts yield a wealth of information about these systems. Within a few seconds, their X-ray brightness increases by a factor of 10 or more, during for a few second to a few minutes, and then decaying to the original level in about a minute. X-ray bursts recur irregularly every few hours or so. Between bursts, new matter flowing from the companion star replenishes the nuclear fuel. That steady accretion gives rise to the persistent emission of X-rays seen between the bursts. Despite the nature of the burst, LMXBs emit more than 90% of their total energy during times of quiescence (*i.e.,* we can see the efficiency of accretion compared to fusion) [vdHea04].

3.2.2 MXRBs and X-ray Pulsars

In MXRBs systems, about half of the objects are *X-ray pulsars*. This is consistent with the idea that a MXRB is the product of the normal evolution of a binary system with a massive star that survived the supernova explosion of its companion. If one of the stars in a close binary system explodes as a supernova, the result may be either a neutron star or a black hole orbiting a companion star.

X-ray pulsars are caused when neutron stars are accompanied by a powerful magnetic field[3]. In fact, these fields may be sufficiently strong to

[2]The X-ray binary with the shortest period discovered to date is 4U1820-30 in the galaxy NGC 6624, with an orbital period of only 11.4 minutes. This source also showed a very long burst of $\sim$ 3 hours [SB02].

[3]Because black holes can have neither a surface nor a strong magnetic field, this account rules them out of consideration as sources of pulsating X-rays [Lew81].

prevent the accreting matter from reaching the star's surface. X-rays are emitted over a large solid angle. If the neutron star's magnetic and rotation axes are not aligned, then the X-ray emitting region may be eclipsed periodically. The result is a *binary X-ray pulsar* [4] [5] [6].

From observations, spectra of millisecond pulsars are usually *non-thermal* (however, they can show thermal spectral components)[Pot14]. Due to this fact and to their large magnetic fields, this category of X-ray bursters is not of interest in this thesis.

3.3 Photospheric Radius Expansion (PRE)

During the outburst of some X-ray bursters, the luminosity can reach a critical limit called the *Eddington limit*, where the radiation pressure exerts a force on the atmosphere that is greater than the gravitational pull. In this case, the photosphere lifts off the surface of the neutron star, and the X-ray bursts lead to the *photospheric radius expansion* (PRE). This phenomenon is a prominent tool to simultaneously measure the neutron star *masses and radii* [vP90], and their implications are discussed in more details in the following chapters.

3.3.1 Eddington Luminosity and Eddington Flux

PRE events occurs when the thermonuclear burning at the bottom of the freshly accreted layer matter can become so powerful that *local luminosity* gets close to the Eddington limit,

$$L_{\rm Edd} = \frac{4\pi GMc}{\kappa_{\rm e}}(1+z_{\rm g}), \tag{3.1}$$

[4] White dwarfs cannot rotate as rapidly as the lower end of this period range without breaking up. This is one indication that X-ray pulsars are accreting neutron stars.

[5] A mechanism capable of producing a binary X-ray pulsar is the accretion-induced collapse of a white dwarf in a close binary system. If the accreting white dwarf could surpass the Chandrasekhar limit without exploding as a *Type Ia supernova*, the resulting gravitational collapse could produce a neutron star that is an X-ray pulsar with a low-mass companion.

[6] X-ray pulsars are powered by the gravitational potential energy released by accreting matter. When mass falls from a great distance to the surface of a neutron star, about 10% of its rest energy is released, an amount that far exceeds the fraction of a percent that would be produced by fusion. The observed X-ray luminosities range up to 10^{38} ergs s^{-1} (the Eddington limit). For a neutron star with a radius of 10 km, the Stefan-Boltzmann equation shows that the temperature associated with this luminosity is about 2×10^7 K. According to the Wien's law, the spectrum of blackbody would peak at X-ray of about 1.5 Å.

where z_g is given by Eq. 2.5 and the *Thomson scattering opacity* is given by

$$\kappa_e \equiv \sigma_T \frac{N_e}{\rho} \sim 0.2\,(1+X)\ \mathrm{cm}^2\ \mathrm{g}^{-1},$$

where $\sigma_T = 6.65 \times 10^{-25}$ cm^2 is the *Thompson cross-section*; ρ is the gas density, N_e is the electron number density; and X is the hydrogen mass fraction by mass of the photospheric matter. The last term of this equation is exact if the opacity is dominated by *electron scattering*.

The total flux emission can be approached to the Eddington (flux) limit if the matter spreads all the way from the equator to the poles. In this case, the spectra present peaks in the same order of magnitude of the Eddington flux,

$$F_{\mathrm{Edd}} = \frac{L_{\mathrm{Edd}}}{4\pi D^2}(1+z_g)^{-2} = \frac{GMc}{\kappa_e D^2}(1+z_g)^{-1}. \tag{3.2}$$

Observationally, the PRE is inferred from the *spectral softening* of the *lightcurve* of the burst. As the photosphere expands, the surface temperature, T_{eff}, decreases. After reaching a minimum, T_{eff} will increase, as the photosphere contracts. The moment when the photosphere falls back to the neutron star surface after the PRE event is called *touchdown*, which is the moment when the *effective temperature*, T_{eff}, reaches its maximum, before decreasing slowly (due to cooling). At the touchdown, the flux is close to the Eddington limit. During the expansion and contraction phase of the photosphere, the local luminosity, as measured by a local observer on the photosphere, remains extremely close to the Eddington luminosity and all the excess flux is converted to kinetic and gravitation potential energy.

PRE events provide information about the neutron star compactness: they give an approximation to the Eddington flux (with a distance dependent mass-radius relation), and the maximum effective temperature of the surface (with a mass-radius relation). Both $T_{\mathrm{eff,max}}$ and F_{Edd} depend on the composition of the atmosphere, as we will see in more details in the following section.

3.3.2 Atmospheric Color Correction Factor (f_c)

The X-ray bursters' atmospheres are said to have *harder* model spectra, which always lie *above* the corresponding blackbody spectra. This is due to the fact that these spectra have more high energy photons than a *softer* model spectra. The hardening of the X-ray spectra is due to the strong

frequency-dependent absorption of the atmosphere, as described in the next chapter[7].

The hardness of the observed (emergent) spectra is evaluated by a multiplicative term called the *color correction factor*, $f_{\rm c}$, which is greater than one. The resulting spectra is named a *diluted blackbody function* with a *color temperature*, $T_{\rm c}$:

$$F \equiv \frac{1}{w_0}\, B(T_{\rm c}), \tag{3.3}$$

where w_0 is the *dilution factor*. This factor is believed to be related to the color correction as $w_0 = f_{\rm c}^{-4}$. In the next chapters, we will obtain f_c and w_0 from our atmospheric models, and we will show results supporting this hypothesis.

The color correction factor is related to the color temperature as:

$$f_{\rm c} \equiv \frac{T_{\rm c}}{T_{\rm eff}}, \tag{3.4}$$

and a first approximation of the color temperature factor suggests that:

$$f_{\rm c} \sim \frac{T\,\text{upper layers}}{T_{\rm eff}}.$$

In addition, the blackbody temperature is the color temperature as seen from an observer at Earth:

$$T_{\rm bb} = T_{\rm c,\infty} = f_{\rm c}\, T_{\rm eff,\infty} = \frac{f_{\rm c} T_{\rm eff}}{(1+z_{\rm g})}.$$

Furthermore, an accurate evaluation of $f_{\rm c}$ depends on the characteristics of the neutron star atmospheres, such as chemical composition and surface gravity. It is also strongly dependent of the luminosity, when close to the Eddington limit [Sul10]. Any of the spectral methods to determine the neutron star masses and radii from X-ray bursters are only possible together

[7] Just as an initial reminder, the emergent emission contains the effects of strong gravity and frequency-dependent *opacities*. At the temperature (millions of kelvins) which produce the X-ray emission observed in neutron star, hydrogen and helium are almost entirely ionized. The dominant term in the opacity is *free-free* absorption, which falls off ν^{-3}. Additionally, *Compton scattering* is an inelastic effect in these atmospheres that does not necessary causes the hardening. Instead, it can even make the spectrum be softer. This is due to the fact that in the rest frame of the electron, the photon loses energy making the stationary electron move. Switching to the *laboratory frame*, the photon could either downscatter or upscatter, depending on parameters such as the speed of the electron or the energy of the photon.

with the determination of these factors for different atmospheric models. These calculations are one of the results of this thesis.

For instance, in the previous discussion about the PREs, it is important to note that a small apparent radius, R_∞, at the touchdown does not mean that the photosphere actually coincides with the neutron star surface. At luminosities very close to Eddington limit, the color correction factors can be rather large. If the touchdown actually meant that the photosphere returned to its original size then the flux would have to be slightly less than $F_{\rm Edd}$ (or the radiation pressure would continue to push the photosphere outward). In many analysis available in the literature, best fits have shown that $F_{\rm touchdown} > F_{\rm Edd}$ [SLB10] [SLB13].

Recently, the *Rossi X-ray Timing Explorer* satellite had over 1400 observations of the 4U 1636-53 low-mass X-ray binary system, and 336 Type I X-ray bursts were identified. From fits to their time-resolved spectra, 69 of these bursts are shown to have PRE bursts. In addition, 17 of these PRE bursts showed that after the touchdown the blackbody radius increases again quickly after 1 second. It was also demonstrated, for the first time, coherent oscillations in the tail of X-ray bursts, which were associated with the behavior of the spectral parameters in that phase of bursts [ZMBH12]. Moreover, the emergence of a deeper theoretical understanding of the atmospheric evolution of X-ray bursters become clear, which is one of the main tasks of this thesis.

3.3.3 The Cooling Phase

We are interested on obtaining simultaneous values for neutron star masses and radii. These values can be used into the *Tolman-Oppenheimer-Volkov* equations to determine the relativistic stellar structure, and reduce the present uncertainty in the equations of state for the cold dense matter [LP01] [Lat07]).

After the touchdown, when the burster photosphere is no longer expanding or contracting, it shows a fast cooling with corresponding variations of the effective temperatures. If the radius of the photosphere is already the same as the radius of the neutron star at this point (by definition, after the touchdown), these variations of $T_{\rm eff}$ can only be explained by variations of $f_{\rm c}$. This fact provides us a powerful tool by using the cooling track to constrain the neutron star parameters.

Moreover, in the cooling phase, we can use the relations:

$$R_\infty = R(1 + z_{\rm g}) = R_{\rm bb} f_{\rm c}^2,$$

to define the *blackbody normalization* of the burster as a function of f_c:

$$K \equiv \left(\frac{R_{bb}}{D} \left[\frac{\text{km}}{10 \text{ kpc}} \right] \right)^2 = \frac{1}{f_c^4} \left(\frac{R(1+z_g)}{D} \left[\frac{\text{km}}{10 \text{ kpc}} \right] \right)^2 = A^4 \frac{1}{f_c^4}, \quad (3.5)$$

where the constant A is defined as the *apparent area* or *normalized emitting area*:

$$A \equiv \left(\frac{R_\infty}{D} \left[\frac{\text{km}}{10 \text{ kpc}} \right] \right)^{-1/2} = \left(\frac{R(1+z_g)}{D} \left[\frac{\text{km}}{10 \text{ kpc}} \right] \right)^{-1/2}, \quad (3.6)$$

which can be used as a spectroscopic quantity since it remains constant while the flux and the blackbody temperature decreases:

$$f = A \, K^{1/4}. \quad (3.7)$$

3.3.4 Application to Observational Data

If an Estimate of the Distance is Available

If we have a precise measure of the object's distance, D (*i.e.,* if one could find a discrete spectral feature in a particular neutron star or the star is located in a globular cluster), the redshift of such object could be directly calculated. With this information, Eq. 3.6 would give all the information needed to uniquely identify the mass and the radius of the neutron star (from Eq. 2.11):

$$M = \frac{c^5}{4G\kappa_e} \frac{A f_c^{-4}}{F_{\infty \text{Edd}}} \left[1 - (1+z_g)^{-2} \right]^2 (1+z_g)^{-3},$$

and

$$R = \frac{c^3}{2\kappa_e} \frac{A f_c^{-4}}{F_{\infty \text{Edd}}} \left[1 - (1+z_g)^{-2} \right] (1+z_g)^{-3}.$$

If an Estimate of the Distance is not Available

Because the evolution of $K^{1/4}$ at the late burst stages reflects the evolution of the color correction factor, we can fit the observationally observed dependence, $K^{-1/4} - F$, to the theoretical parameters obtained from simulations, $f_c - l$ [Sul10]. The two free parameters are A and F_{Edd}, and combining them, we obtain a relation for the *effective* temperature corresponding to

the Eddington flux on the neutron star surface, corrected for the surface gravity:

$$T_{\mathrm{Edd},\infty} = \Big(\frac{gc}{\sigma_{\mathrm{SB}}\kappa_{\mathrm{e}}}\Big)^{1/4}\frac{1}{1+z_{\mathrm{g}}} = 6.4\times10^{9}\,F_{\mathrm{Edd}}^{1/4}\,A^{-1}\,K.$$

With this quantity, which is independent of the distance, we can express the neutron star radius and mass through the compactness factor (Eq. 2.3):

$$R = \frac{c^3}{2\kappa_{\mathrm{e}}\sigma_{\mathrm{SN}}T_{\mathrm{Edd},\infty}^4}c_{\mathrm{g}}(1-c_{\mathrm{g}})^{3/2}, \tag{3.8}$$

and

$$M = \frac{R}{2.95[\mathrm{km}]}\,c_{\mathrm{g}}\,M_{\odot}. \tag{3.9}$$

Chapter 4

Atmospheric Opacities of Neutron Stars

The atmospheric *opacity* of neutron stars is determined by the details of how photons interact with particles (atoms, ions, free electrons). Both absorption and scattering remove photons from a beam of light, and contribute to the opacity. In general, it is a function of composition, density, and temperature. In this section we will study these processes in more details.

4.1 Opacity Sources

In general, there are four primary sources of opacity available for removing stellar photons from a beam. Each involves a change in the quantum state of an electron:

- **Bound-bound transitions**, $\kappa_{\nu,\mathrm{bb}}$: When an electron in an atom or ion makes a transition from one orbital to another. An electron makes an upward transition from a lower to a higher orbit when a photon of the appropriate energy is absorbed. The bound-bound opacity is significant only at the discrete frequencies that allow upward atomic transition. This is the opacity responsible for forming the absorption lines in the stellar spectra. The reverse emission process occurs when the electron makes a downward transition from a higher to a lower orbit. The net result of this absorption-emission sequence is essentially a scattered photon. A by-product of this absorption process is the degradation of the average energy of the photons in the radiation field.

- **Bound-free absorption**, $\kappa_{\nu,\mathrm{bf}}$: Also know as *photoionization*, occurs when an incident photon has enough energy to ionize an atom. The resulting free electron can have any energy, so any photon with a wavelength $\lambda \leq hc/\epsilon_n$, where ϵ_n is the ionization energy of the nth orbital, can remove an electron from an atom. The bound-free opacity is one source of the continuum opacity. The cross section for the photoionization of a hydrogen atom in quantum state n by a photon of wavelength λ is:

$$\sigma_{\mathrm{bf}} = 1.31 \times 10^{-15} \frac{1}{n^5} \Big(\frac{\lambda}{5000\,\text{Å}} \Big)\ \mathrm{cm}^2.$$

  The inverse process of free-bound emission occurs when a free electron recombines with an ion, emitting one or more photons in random directions. This opacity also contributes to reduce the average energy of the photons in the radiation field.

- **Free-free absorption**, $\kappa_{\nu,\mathrm{ff}}$: It is a scattering process when a free electron is in the vicinity of an ion and absorbs a photon, causing the speed of the electron to increase. This can happen over a continuous range of wavelengths, therefore this opacity is another contributor to the continuum opacity. It may also happen that the electron loses energy as it passes near an ion by emitting a photon, causing the electron to slow down as a result. This process of free-free emission is known as *bremsstrahlung emission*.

- **Electron scattering**, κ_{es}: A photon is scattered by a free electron through the process of *Thompson scattering*. The cross section for Thomson scattering, σ_T, has the same value for photons of all wavelengths. The small size of the Thomson cross section means that electron scattering is most effective as a source of opacity at high temperatures. In atmospheres of the neutron stars where, most of the gas is completely ionized, other sources of opacity that involve bound electrons are eliminated. In this high temperature regime, the opacity due to electron scattering dominates the continuum opacity.

- **Compton scattering and Rayleigh scattering**: A photon may also be scattered by an electron that is loosely bound to an atomic nucleus. This result is called Compton scattering if the photons wavelength is much smaller than the atom, and Rayleigh scattering if the photons wavelength is much larger. Rayleigh scattering is proportional to $1/\lambda^4$ and can be neglected in most atmospheric models.

The primary source of the continuum opacity in most stellar atmospheres is the photoionization of H^- ions, since the assemble of two electrons orbiting a single proton has a ionization of only $\epsilon = 0.754$ eV. This means that any photon with wavelength $\lambda \leq \frac{hc}{\epsilon} = 16400$ Å can remove an electron from the ion. H^- ions become increasingly ionized at higher temperatures and at higher temperature, the photoionization of helium also contributes to the opacity.

4.1.1 Rosseland Mean Opacity

The total opacity is the sum of the opacities due to all the aforementioned sources is given by:

$$\kappa_\lambda = \kappa_{\lambda,\mathrm{bb}} + \kappa_{\lambda,\mathrm{bf}} + \kappa_{\lambda,\mathrm{ff}} + \kappa_{\mathrm{es}}$$

This result depends on the wavelength (or frequency) of the light being absorbed, together with the composition, density, and surface gravity of the atmosphere (*e.g.,* the electron number density, the states of excitation and ionization of the atoms and ions).

The opacity that has been averaged over all wavelengths results in a function of only the composition, density, and temperature. This average opacity, $\bar{\kappa}$, is known as the *Rosseland mean opacity.*

There is no simple equation to describe all the individual spectral lines in the bound-bound transitions. For the average bound-free opacity, an approximation formula is:

$$\bar{\kappa}_{\mathrm{bf}} = 4.34 \times 10^{25}\ \frac{g_{\mathrm{bf}}}{t}\ Z(1+X)\ \frac{\rho}{T^{3.5}}\ \ [\mathrm{cm^2 g^{-1}}],$$

where ρ is the density in g cm^{-3}; T is temperature in kelvin; X and Z are the fractional abundances (by mass) of hydrogen and metals respectively; and the correction factor, t, is the *guillotine factor*, describing describe the cutoff of an atom's contribution of the opacity after it has been ionized.

For free-free opacities, we have:

$$\bar{\kappa}_{\mathrm{ff}} = 3.68 \times 10^{22}\ g_{\mathrm{ff}}(1-Z)(1+X)\ \frac{\rho}{T^{3.5}}\ \ [\mathrm{cm^2 g^{-1}}].$$

The *Gaunt factors*, g_{bf} and g_{ff}, are quantum mechanical correction terms and are both ~ 1 for the visible and ultraviolet wavelengths. It lies between 1 and 100. Note that both formulas have the functional:

$$\bar{\kappa} = \frac{\kappa_0 \rho}{T^{3.5}},$$

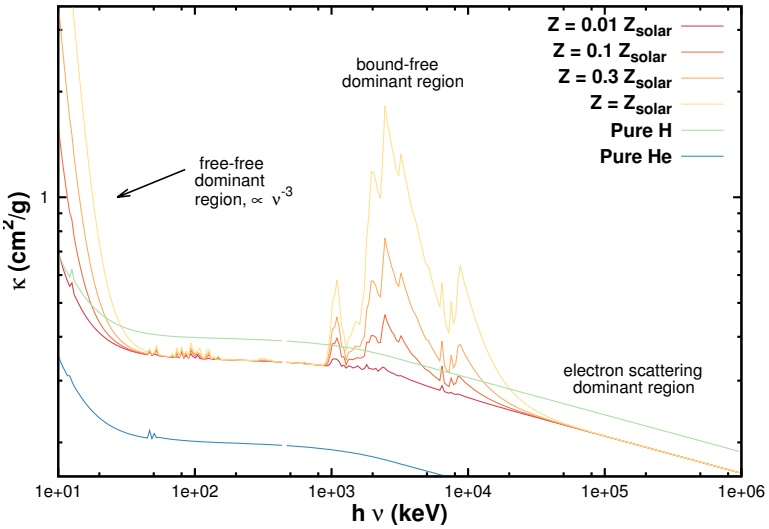

Figure 4.1: This figure shows the Rosseland opacities' dependence on the energy for the LANL opacities. We can see that at low photon energies, the free-free opacities are dominant over electron scattering.

where κ_0 is a constant. Any opacity with density and temperature dependence obeys the *Kramers opacity law* [Kra23].

Because the cross section for electron scattering is independent of the frequency or wavelength, the Rosseland mean for this case is:

$$\kappa_e = 0.2(1 + X) \ \ [\mathrm{cm}^2\ \mathrm{gm}^{-1}].$$

The final Rosseland mean opacity $\bar{\kappa}$ is the average of the sum of the individual contributors to the opacity:

$$\bar{\kappa} = \kappa_{\mathrm{bb}} + \kappa_{\mathrm{bf}} + \kappa_{\mathrm{ff}} + \kappa_{\mathrm{es}}.$$

4.2 Basic Concepts for Neutron Star Atmospheres

As we highlighted in the previous chapters, neutron star spectra deviate from the blackbody function. For this reason, finding the surface temperature of a particular star can be a complicated task. There are different ways of defining the temperature of a star:

- Effective temperature (from the Stefan-Boltzmann relation, Eq. 2.2).

- Excitation temperature (from the Boltzmann equation, Eq. 1.9).
- Ionization temperature (from the Saha equation Eq. 1.10).
- Kinetic temperature (from the Maxwell-Boltzmann distribution, Eq. 1.8).
- Color temperature (by fitting the shape of a stars continuous spectrum to the blackbody function, Eq. 3.4).

These temperatures are the same for a gas confined within a box because the blackbody radiation will come into equilibrium. In such steady-state condition, no net flow of energy through the box or between the matter and radiation occurs. Every process (*e.g.,* absorption of a photon) occurs a the same rate as the inverse process (*e.g.,* emission of a photon). This is called *thermodynamic equilibrium.*

4.2.1 Local Thermodynamic Equilibrium

A star cannot be in a perfect hydrodynamic equilibrium. A net outward flow of energy occurs through the star surface and the temperature varies with location on that boundary. As the gas particles collide with one another and interact with the radiation field by absorbing and emitting photons, the description of the processes of excitation and ionization becomes quite complex. However, the idealized case of a single temperature can be employed if the distance over which the temperature changes significantly is large when compared with the distances traveled by the particles between collisions (*i.e.,* their *mean free paths*). This is *local thermodynamic equilibrium* (LTE), which states that particles and photons cannot escape the local environment and so are effectively confined to a limited volume of nearly constant temperature.

4.2.2 Mean Free Paths and Opacity

Consider a beam of parallel light rays traveling through a gas. Any process that removes photons from a beam of light is called *absorption.* This includes *scattering of photons* (Compton scattering) and *absorption of photons* by atomic electrons making upward transitions.

The change in the intensity, dI_ν, of a ray of frequency ν as it travels through the gas is proportional to its intensity; the distance traveled, ds; and the density of the gas, ρ:

$$dI_\nu = -\kappa_\nu \rho I_\nu ds. \tag{4.1}$$

where the quantity κ_ν is the frequency-dependent opacity.

The distance is measured along the path traveled by the beam and increases in the direction that the beams travel, the minus sign in the equation above shows that the intensity decreases with distance due to the absorption of photons.

The final intensity after light has traveled a distance s is found by integrating Eq. 4.1. For a uniform gas with constant opacity and density, we have:

$$I_\nu = I_{\nu,0}\, e^{-\kappa_\nu \rho s}.$$

We see that the intensity declines exponentially falling by a factor of e^{-1} over the characteristic distance of $l = 1/\kappa_\nu \rho$. Thus, for scattered photons, the *mean free path of photons* is defined as:

$$l = \frac{1}{\kappa_\nu \rho} = \frac{1}{n\sigma_\nu}$$

.

4.2.3 Optical Depth

When observing the light from a star, we are looking back along the path traveled by the photons. The *optical depth* of a light ray can be defined as the number of mean free paths passed from the original position to the surface, and written as:

$$d\tau_\nu = -\kappa_\nu \rho ds.$$

If the optical depth of the light ray starts at the point $\tau_\nu = 1$, the intensity of the ray will decline by a factor of e^{-1} before escaping from the star. If $\tau_\nu \gg 1$ for a light ray passing through a volume of gas, the gas is said to be optically thick. If $\tau_\nu \ll 1$, the gas is optically thin. Because the optical depth varies with wavelength, a gas may be optically thick at one wavelength and optically thin at another[1].

4.2.4 Random Walk and Displacement

In equilibrium, neutron star atmospheres do not exhibit any change in the total energy. Absorption and emission of energy must be precisely in balance (any process that adds photons to a beam of light is called emission). The processes of absorption and emission redirect the paths and energies of the photons in the atmosphere. The individual photons travel only

[1]For instance, the Earth's atmosphere is optically thin at visible wavelengths and thick to X-ray wavelengths.

temporarily with the beam since they are repeatedly scattered in random directions.

The transport of energy through a star by radiation is in general very inefficient. As the photon diffuses upward through the stellar material, it follows the so-called *random walk*, which is a large number, N, of randomly direct steps, each of length, l. From statistical mechanics, the displacement, d, is related to the size of each step, l, as $d = l\sqrt{N}$. While the distance to the surface is $d = \tau_\lambda l = l\sqrt{N}$, the average numbers of steps that a photon takes to leave the surface (traveling d) is $N = \tau_\lambda^2$, for $\tau_\lambda \gg 1$.

4.2.5 Radiation Pressure

The temperature of the neutron star atmosphere decreases with increasing radius, thus the radiation pressure is smaller when far from the center. The gradient in the radiation pressure produces the movement of photons towards the surface that carries the radiative flux:

$$\frac{dP_{\rm rad}}{dr} = -\frac{\bar{\kappa}\rho}{c}\, F_{\rm rad},$$

The transfer of energy by radiation is a process involving the upward diffusion of randomly walking photons, drifting toward the surface in response to the gradient in the radiation pressure.

4.2.6 Radiation Intensity

The increase of the radiation intensity, dI_ν, is proportional to ds and to ρ. It also changes as the photons within the beam are removed by absorption or are replaced by photons emitted from the surrounding material. Considering the decrease in intensity due to absorption to the pure emission, we have:

$$dI_\nu = -\kappa_\nu \rho I_\nu ds + j_\nu \rho ds, \tag{4.2}$$

where j_ν [cms^{-3}sr^{-1}] is the emission coefficient of the gas (which varies with wavelength).

4.2.7 The Transfer Equation

The rates at which the processes of emission and absorption compete determines how fast the radiation intensity changes. It can be obtained by dividing Eq. 4.2 by $-\kappa_\nu \rho ds$:

$$-\frac{1}{\kappa_\nu \rho}\frac{dI_\nu}{ds} = I_\nu - \frac{j_\nu}{\kappa_\nu},$$

where $S_\nu = \frac{j_\nu}{\kappa_\nu}$ it is called source function and describes how photons within the beam are removed and replaced by photons from the surrounding gas. In thermodynamic equilibrium, the source function is equal to the blackboard function, $S_\nu = B_\nu$ (intensity is constant). At a depth where the photon mean free path is small compared to a limited volume, local thermodynamic equilibrium (LTE) is satisfied and the source function is equal to the Planck function.

Moreover, we can rewrite the transfer equation in terms of the optical depth as:

$$\frac{dI_\nu}{d\tau_\nu} = I_\nu - S_\nu.$$

The optical depth should be replaced by a meaningful measure of position. A *vertical optical depth*, $\tau_{\nu,v}(z)$ is defined as:

$$\tau_{\nu,v}(z) = \int_z^0 \kappa_\nu \rho dz.$$

Thus, the transfer equation can be rewritten as:

$$\cos\theta \frac{dI_\nu}{d\tau_{\nu,v}} = I_\nu - S_\nu$$

This form of the transfer equation is employed when dealing with the approximation of a *plane-parallel atmosphere*. The opacity can be assumed to be independent of wavelength if you take it to be equal to the Rosseland mean opacity, $\bar{\kappa}$. A stellar atmosphere in which the opacity is assumed to be independent of wavelength is considered a *gray atmosphere*, reflecting its indifference to the spectrum of wavelengths.

The assumption of a gray atmosphere is good for the majority of stars for which the photoionization of H^- ions is the primary source of opacity, because the opacity does not vary rapidly with wavelength. If we write $\bar{\kappa}$ instead of κ, the vertical optical depth no longer depends on wavelength. The remaining wavelength dependencies may be removed by integrating the transfer equation over all wavelengths.

4.3 Brief History of Atmospheric Models

In the past three decades, a range of neutron star atmosphere models were made available in the literature. They present the dependence of the *emergent surface flux*[2] versus the frequency (or energy) of the photons.

[2]For some authors, the flux is presented over 4π, referenced as H_E.

Atmospheric calculations are based on parameters such as *chemical composition* (*e.g.,* the hydrogen mass fraction X and solar mixings) and *surface gravity, g,* (Eq. 2.4). In general, these models assume *plane-parallel* approximation for the photosphere and the equation of state of an ideal gas in *local thermodynamic equilibrium* (LTE). The structure of the atmosphere is described by a set of differential equations for the *hydrostatic* and *radiation* equilibrium. Moreover, for convenience, we can define the *relative surface luminosities* in terms of the Eddington luminosity and the effective temperature, Eqs. 3.1 and 2.2, as:

$$l = \frac{L}{L_{\rm Edd}} = \left(\frac{T_{\rm eff}}{T_{\rm Edd}} \right)^4 . \tag{4.3}$$

London et al. [Lon86] implemented the first detailed numerical calculation of atmospheric models of a non-magnetic neutron star that included *comptonization*, *free-free* processes (due to ionized hydrogen and helium), and *bound-free absorption* (due to K shell transitions from Fe^{+24} to Fe^{+25}), as sources to atmospheric *opacity*. In addition, they claimed that bound-free transitions were not important for bursts close to the Eddington limit. They used the *Kompaneets operator* to describe the Compton scattering in the non-relativistic and isotropic diffusion approximation, which was claimed to be adequate for hot neutron star model atmospheres with *effective temperatures below* ~ 2 *keV*. Energy transport mechanism besides radiation (*e.g.,* convection) were negligenced. They present an investigation of the radiative transfer of the neutron star photosphere for *17 different models*, with *effective temperatures ranging from 0.25 to 3 keV*, *surface gravities* $\log g =$ *14 and 15* (in cgs units), and *helium and iron abundances (Fe/H) from 0 to 1 relative to solar abundance*. They assumed that the atmospheres were in a steady state and in radiative equilibrium, justified by the fact that the hydrodynamical and thermal time scales within the atmosphere are much shorter than the time scales over which the observed fluxes vary. They found that the spectrum significantly differed from a blackbody radiating at the effective temperature and the differences were associated to effects from *surface cooling*. With luminosity ratios (Eq. 4.3) not exceeding 0.8, they obtained *color correction factors* in the range $1.39 < f_{\rm c} < 1.76$.

In the following year, Ebisuzaki [Ebi87] analytically described the atmospheric structures of X-ray bursters, comparing his models to two observed sources, MXB 1636-536 and MXB 1608-522. He assumed that the spectrum deviates from a blackbody due to Compton heating and cooling. He obtained relations for mass, radius and distance of the bursters, deriving two

possible sets of these parameters, taking into account the 4-1 keV absorption line, which would be due Cr XXIII ($M = 1.7 - 2.0 M_{\odot}, R = 11 - 12$ km and $D = 6.3 - 6.7$ kpc) or due Fe XXV ($M = 1.8 - 2.1 M_{\odot}, R = 8 - 10$ km and $D = 5.8 - 6.4$ kpc). In his calculations, he assumed *color-correction factor* of $f_{\rm c} = 1.34$, $0.3 < l < 0.95$, and that the surface of the neutron star was covered with *pure helium matter* in the decay phases, without any heavy elements and neglecting any bound-free opacities. His results revealed that an isothermal outer layer with $T > T_{\rm eff}$ is formed in the photosphere due to Compton heating of electrons by hot photons coming from deeper layers.

Pavlov et al. [Pav91] developed a numerical model of the photosphere of X-ray bursts when the bursters are very close to the Eddington limit, with relative luminosities (Eq. 4.3) ranging $0.9 \leq l \leq 0.999$. They considered *electron scattering* and *free-free transitions*, assuming that the photosphere consists of hydrogen and helium. Their results showed a diluted spectrum for the burster atmosphere, with spectral temperature coinciding to the electron temperature in an isothermal outer layer formed by Compton heating . The *dilution factor* was proportional to $f_{\rm c}^4$.

In 2004, Madej et al. [Mad04] presented 47 atmosphere models of very hot neutron stars, where the process of scattering of photons by free electrons was approximated by *coherent* and *isotropic* photoelectric collision. They used the integral description of Compton scattering, employing an *angle-averaged redistribution function.* The resulting flux spectrum of the outgoing radiation took into the account all the *bound-free* and *free-free* monochromatic opacities relevant to the hydrogen-helium chemical compositions, *i.e.,* the effects of *Compton scattering* of radiation in the thermal plasma with fully relativistic thermal velocities. Their hydrogen-helium model atmospheres and flux spectra were computed on a range of *effective temperature* from 1×10^7 K to 3×10^7 K, and with only one value for surface gravity, $\log g = 15.0$. They found that *all color correction factors were consistently smaller than* 1.9. The group calculated values for the neutron star masses and radii from a direct fitting of the observed X-ray burst spectrum, proposing a best-fit for a fixed $\log g$ and varying l (or T_{eff}) and the gravitational redshift z. The best-fit between all trial $\log g$ values would give the desired g and z, and the mass and radii would be found by the Eq. 2.10. However, the curves on the $M - R$ planes to the fixed $\log g$ and z reproduced very large uncertainties. In a following paper, [Maj05], they adopted the same equations to calculate 106 models including iron ions and adding dozen bound-bound opacities for the highest ions of the iron. Their results differed significantly from pure hydrogen-helium spectra and from the blackbody spectra, with *color correction factors* $1.2 < f_{\rm c} < 1.85$.

Recently, Suleimanov et al. [Sul10] adopted the *differential Kompaneets operators* to consider the Compton scattering in 360 atmospheric models (instead of the more general integral operator for the Compton scattering kernel). They solved the radiation transfer equation and the hydrostatic equilibrium equation accounting for the radiation pressure by electron scattering. Their models were computed for *six chemical compositions* (pure helium, pure hydrogen, solar hydrogen/helium mix with various heavy elements abundances, Z=1,0.3, 0.1 and 0.01 $Z_{\odot}$), and *three surface gravities* $\log g = 14.0, 14.3$, and 14.6, with relative luminosities ranging from $0.001 \leq l \leq 0.98$. They calculate the redshifts from $\log g$, by adopting a neutron mass equal to $1.4 M_{\odot}$ for $\log g = 14.0, 14.3, 14.6$ and getting $R = 14.8, 10.88, 8.16$ and $z = 0.18, 0.27, 0.42$. The emergent spectra of all the models were redshifted and fitted by a diluted blackbody within 3-20 keV (RXTE/PCA range). They also suggested a new method for the determination of the neutron star radii and masses, at late phases of PRE X-ray bursts, based on the spectral (blackbody) normalization K, Eq. 3.5 and depending only on the color correction factor. Suleimanov et al. (2012) [Sul12] extended their neutron star atmosphere to 484 models (and l up to $1.06-1.1$) using, for the first time, an *exact treatment of Compton scattering via the integral relativistic kinetic equation.* In the new approach, the *Klein-Nishima reduction* in the electron scattering cross-section led to a decrease in the radiative acceleration relative to that for the Thomson scattering cross-section. The values of the color correction factor for the new models with $l < 0.8$ were almost identical to the old models based on Kompaneets operator. However, the comparison to [Mad04] showed dramatic differences in the spectral shape.

Bibliography

[Bil00] L. Bildsten. Theory and observations of Type I X-Ray bursts from neutron stars. In S. S. Holt and W. W. Zhang, editors, *American Institute of Physics Conference Series*, volume 522 of *American Institute of Physics Conference Series*, pages 359–369, June 2000.

[Bol72] L Boltzmann. *Weitere Studien ber das Wrmegleichgewicht unter Gasmoleklen*, wiener berichte, 66, 275-370, i, 316-402. 1872.

[Bol84] L Boltzmann. *Ableitung des Stefan'schen Gesetzes, betreffend die Abhngigkeit der Wrmestrahlung von der Temperatur aus der electromagnetischen Lichttheorie*, annalen der physik und chemie, bd. 22, s. 291-294. 1884.

[BV81] E. Bohm-Vitense. *The Effective Temperature Scale*, annu. rev. astro. astrophys. 1981.

[Car96] BW Carroll. *An Introduction to Modern Astrophysics*, addison-wesley publishing compamy, inc. 1996.

[Cav77] Maraschi & Cavaliere. *X-Ray Bursts of Nuclear Origin*, international astronomical union / union astronomique internationale volume 4-1, 1977, pp 127-128. 1977.

[CF53] S Chandrasekhar and E Fermi. *Problems of Gravitational Stability in the Presence of a Magnetic Field. The Astrophysical Journal*, 118(116), 1953.

[Com23] AH Compton. *A Quantum Theory of the Scattering of X-Rays by Light Elements*, physical review 21 (5): 483502. 1923.

[deB24] L deBroglie. *Recherches sur la Theorie des Quanta*. 1924.

[Ebi87] T Ebisuzaki. *PASJ*, 39:287, 1987.

[Ein05a] A Einstein. *Zur Elektrodynamik bewegter Krper*, annalen der physik, bern. 1905.

[Ein05b] A Einstein. *ber einen die Erzeugung und Verwandlung des Lichtes betreffenden heuristischen Gesichtspunkt*, annalen der physik 17 (6): 132148. 1905.

[Fea78] W Forman et al. *HEASARC archive for Uhuru*, apjs, 38, 357. 1978.

[Gut97] A Guth. *The Inflationary Universe*. 1997.

[Hea80] J.H. Helfand et al. *Thermal X-ray Emission from Neutron Stars*, nature vol. 283 24. 1980.

[Her88] HR Hertz. *Ueber die Ausbreitungsgeschwindigkeit der electrodynamischen Wirkungen*, annalen der physik, vol. 270, no. 7, p. 551569, may. 1888.

[Hor75] Hansen & Van Horn. Apj 195, 735. 1975.

[Huy90] C Huygens. *Trait de la Lumiere*. 1690.

[JKR01] H.-T. Janka, K. Kifonidis, and M. Rampp. Supernova Explosions and Neutron Star Formation. In D. Blaschke, N. K. Glendenning, and A. Sedrakian, editors, *Physics of Neutron Star Interiors*, volume 578 of *Lecture Notes in Physics, Berlin Springer Verlag*, page 363, 2001.

[Jos76] P.C. Joss. *The X-ray bursters*, nature vol.264 november 18. 1976.

[Jos80] Lewin & Joss. *X-ray Bursters and the X-ray Sources of the Galactice Bulge*, space science reviews 28 (1981) 3-87. 1980.

[Kra23] HA Kramers. *On the Theory of X-ray Absorption and of the Continuous X-ray Spectrum*, philosophical magazine 46: 836. 1923.

[Lat07] James M Lattimer. Equation of state constraints from neutron stars. In *Isolated Neutron Stars: From the Surface to the Interior*, pages 371–379. Springer Netherlands, 2007.

[Lew77] W.H.G. Lewin. *X-ray Burst Sources*, nature vol. 270 17. 1977.

[Lew81] W.H.G. Lewin. *The Sources of Celestial X-ray Bursts*, scientific american. 1981.

[Lew93] W.H.G. Lewin. *X-ray Bursts*, space science reviews 62: 223-389,1993. 1993.

[Lon86] Taam R.E. & Howard W.M London, R. A. *ApJ*, 170:1986, 1986.

[LP01] JM Lattimer and M Prakash. Neutron star structure and the equation of state. *The Astrophysical Journal*, 550(1):426, 2001.

[Mad04] Joss P.C. & Rozanska Madej, J. *ApJ*, 602:904, 2004.

[Maj05] Madej J. Joss P. C. & Rozanska A. Majczyna, A. *ApJ*, 430:643, 2005.

[Max59] L Maxwell. *On the Dynamical Theory of Gases. Phil. Mag. 19:434-36, 1860; in: Scientific Letters, Vol. I. (pg. 616)*, 1859.

[Max61] L Maxwell. *On Physical Lines of Force*. 1861.

[Mis73] Thorne K.S. & Wheeler J.A. Misner, W.C. *Gravitation. Publisher: W. H. Freeman*, 1973.

[NIS14] NIST. *The NIST Reference om Constants, Units, and Uncertainty*, http://physics.nist.gov/cgi-bin/cuu/value?bwien. 2014.

[Pad93] T Padmanabhan. *Structure Formation in the Universe*, cambridge university press. 1993.

[Pav91] Shibanov I.A. & Zavlin Pavlov, G. G. *MNRAS*, 253:287, 1991.

[PGC11] J. M. Pearson, S. Goriely, and N. Chamel. Properties of the outer crust of neutron stars from hartree-fock-bogoliubov mass models. *Phys. Rev. C*, 83:065810, Jun 2011.

[Pla01] M Planck. *On the Law of Distribution of Energy in the Normal Spectrum*, annalen der physik, vol. 4, p. 553 ff. 1901.

[Pot14] A. Y. Potekhin. Atmospheres and radiating surfaces of neutron stars. *ArXiv e-prints*, March 2014.

[Ros73] M Rosenbluth. Ap. j. 184 : 907. 1973.

[Sah21] MN Saha. *On a Physical Theory of Stellar Spectra*, proceedings of the royal society a: Mathematical, physical and engineering sciences 99 (697): 135. 1921.

[SB02] T. E. Strohmayer and E. F. Brown. A Remarkable 3 Hour Thermonuclear Burst from 4U 1820-30. *ApJ*, 566:1045–1059, February 2002.

[SB03] T. Strohmayer and L. Bildsten. New Views of Thermonuclear Bursts. *ArXiv Astrophysics e-prints*, January 2003.

[Sea83] S.L. Shapiro et. al. *Black Holes, White Dwarfs and Neutron Stars: The Physics of Compact Objects*. 1983.

[SLB10] Andrew W Steiner, James M Lattimer, and Edward F Brown. The equation of state from observed masses and radii of neutron stars. *The Astrophysical Journal*, 722(1):33, 2010.

[SLB13] A. W. Steiner, J. M. Lattimer, and E. F. Brown. The Neutron Star Mass-Radius Relation and the Equation of State of Dense Matter. *ApJ*, 765:L5, March 2013.

[Ste79] J Stefan. *Uber die Beziehung zwischen der Warmestrahlung und der Temperatur, in: Sitzungsberichte der mathematisch*, akademie der wissenschaften, bd. 79 (wien 1879), s. 391-428. 1879.

[Sul10] Poutanen J. & Werner K. Suleimanov, V. *A&A*, 527:A139, 2010.

[Sul12] Poutanen J. & Werner K. Suleimanov, V. *A&A*, 545:A120, 2012.

[vdHea04] E.P.J. van den Heuvel et al. *X-ray Binaries*, scientific american. 2004.

[vP78] J van Paradijs. *Nature* 274 650. 1978.

[vP90] et al. van Paradijs, J. *A&A*, 235:156, 1990.

[Wam79] W Wamsteker. *Observational Constraints on the Masses of Neutron Stars*, so messenger, sept. 1979, p. 31-33. 1979.

[Wei93] S Weinberg. *The First Three Minutes: A Modern View Of The Origin Of The Universe*. 1993.

[Wie98] W Wien. *Ueber die Fragen, welche die translatorische Bewegung des Lichtthers betreffen*, annalen der physik 301 (3): Ixviii. 1898.

[WIS14] WISC. *Physical Constants and Astronomical Data*, http://www.astro.wisc.edu/ dolan/constants.html. 2014.

[WT76] S.E. Woosley & Taam. *Gamma-ray bursts from thermonuclear explosions on neutron stars*, nature, 263, 101. 1976.

[Zea96] V.E. Zavlin et al. *Astron. Astrophys.* 315 141. 1996.

[ZMBH12] Guobao Zhang, Mariano Mendez, Tomaso M Belloni, and Jeroen Homan. Coherent oscillations and the evolution of the emission area in the decaying phase of radius-expansion bursts from 4u 1636-53. *arXiv preprint arXiv:1204.3486*, 2012.

Index